

 Open access • Journal Article • DOI:10.1021/ACS.JPCC.5B06428

Promising Piezoelectric Performance of Single Layer Transition-Metal Dichalcogenides and Dioxides — [Source link](#)

M. Menderes Alyörük, Yierpan Aierken, Deniz Çakır, François M. Peeters ...+1 more authors





Institutions: University of Antwerp, Anadolu University

Published on: 24 Sep 2015 - Journal of Physical Chemistry C (American Chemical Society)

Topics: Piezoelectricity

Related papers:

- [Intrinsic Piezoelectricity in Two-Dimensional Materials](#)
- [Ab Initio Prediction of Piezoelectricity in Two-Dimensional Materials.](#)
- [Observation of piezoelectricity in free-standing monolayer MoS2](#)
- [Generalized Gradient Approximation Made Simple](#)
- [Piezoelectricity of single-atomic-layer MoS2 for energy conversion and piezotronics.](#)

Share this paper:    

View more about this paper here: <https://typeset.io/papers/promising-piezoelectric-performance-of-single-layer-45a9w3eilj>

This item is the archived preprint of:

Promising piezoelectric performance of single layer transition-metal dichalcogenides and dioxides

Reference:

Alyoruk M. Menderes, Aierken Yierpan, Çakir Deniz, Peeters François, Sevik Cem.- Promising piezoelectric performance of single layer transition-metal dichalcogenides and dioxides

The journal of physical chemistry: C: nanomaterials and interfaces - ISSN 1932-7447 - 119:40(2015), p. 23231-23237

Full text (Publishers DOI): <http://dx.doi.org/doi:10.1021/acs.jpcc.5b06428>

To cite this reference: <http://hdl.handle.net/10067/1294180151162165141>

Promising piezoelectric performance of single layer transition-metal dichalcogenides and dioxides

M. Menderes Alyörük,^{*,†} Yierpan Aierken,^{*,‡} Deniz Çakır,^{*,‡} Francois M. Peeters,^{*,‡} and Cem Sevik^{*,¶}

Department of Computer Education and Instructional Technologies, Dumlupınar University, Kütahya, Turkey., Department of Physics, University of Antwerp, Groenenborgerlaan 171, B-2020, Antwerpen, Belgium., and Department of Mechanical Engineering, Anadolu University, Eskişehir, TR 26555, Turkey.

E-mail: menderes.alyoruk@dpu.edu.tr; yierpan.aierken@uantwerpen.be; dcakir79@gmail.com; francois.peeters@uantwerpen.be; csevik@anadolu.edu.tr

Abstract

Piezoelectricity is a unique material property that allows one to convert mechanical energy into electrical one or vice versa. Transition metal dichalcogenides (TMDC) and transition metal dioxides (TMDO) are expected to have great potential for piezoelectric device applications due to their non-centrosymmetric and two-dimensional crystal structure. A detailed theoretical investigation of the piezoelectric stress (e_{11}) and piezoelectric strain (d_{11}) coefficients of single layer TMDCs and TMDOs with chemical

*To whom correspondence should be addressed

[†]Department of Computer Education and Instructional Technologies, Dumlupınar University, Kütahya, Turkey.

[‡]Department of Physics, University of Antwerp, Groenenborgerlaan 171, B-2020, Antwerpen, Belgium.

[¶]Department of Mechanical Engineering, Anadolu University, Eskişehir, TR 26555, Turkey.

formula MX_2 (where $\text{M} = \text{Cr, Mo, W, Ti, Zr, Hf, Sn}$ and $\text{X} = \text{O, S, Se, Te}$) is presented by using first-principles calculations based on density functional theory. We predict that not only the Mo and W based members of this family but also the other materials with $\text{M} = \text{Cr, Ti}$ and Sn exhibit highly promising piezoelectric properties. CrTe_2 has the largest e_{11} and d_{11} coefficients among the group VI elements (i.e., Cr, Mo and W). In addition, the relaxed-ion e_{11} and d_{11} coefficients of SnS_2 are almost the same as those of CrTe_2 . Furthermore, TiO_2 and ZrO_2 pose comparable or even larger e_{11} coefficients as compared to Mo and W based TMDCs and TMDOs. Our calculations reveal that TMDC and TMDO structures are strong candidates for future atomically thin piezoelectric applications such as transducers, sensors and energy harvesting devices due to their piezoelectric coefficients that are comparable (even larger) to currently used bulk piezoelectric materials.

1 Introduction

Semiconductor transition metal dichalcogenides (TMDC) and transition metal dioxides (TMDO) have received significant interest due to their potential usage in future nanoelectronic and nanophotonic applications.¹⁻⁹ In particular, the discovery and characterization of a large number of different layered semiconductor materials with distinctive physical and chemical properties has increased this interest further. Until now, the electronic, magnetic and vibrational properties of a large number of TMDC compounds have been investigated theoretically by using, in particular, first principles calculations.^{10,11} Furthermore, extensive experimental studies have shown that single or few layers of MX_2 ($\text{M} = \text{Mo, W}$ and $\text{X} = \text{S, Se, Te}$) structures¹²⁻¹⁹ have remarkable potential for diverse technological applications such as, in catalysis,²⁰ energy-storage,²¹ sensing,²² field-effect transistors^{12,18,23,24} and logic circuits,^{22,25} due to their wide-range tunability by doping, strain or electric field engineering.

In addition to these exciting applications, that are based on their non-centrosymmetric structures, TMDCs in the 2H crystal structure with D_{3h} symmetry have also been shown to

have remarkable piezoelectric properties that has triggered their use in pressure sensors,²⁶ transducers,²⁷ high voltage generators,²⁸ nonlinear energy harvesters²⁹ and energy conversion and piezotronic applications.³⁰ Recently, few studies have focused on the piezoelectric properties of the TMDC^{31,32} and other 2D structures.^{33–36} Duerloo *et al.* calculated the piezoelectric properties of single layer of BN, MoS₂, MoSe₂, MoTe₂, WS₂, WSe₂, and WTe₂ by using first principle calculations.³¹ They reported that relaxed-ion piezoelectric strain (d_{11}) and piezoelectric stress (e_{11}) coefficients of the 2H-TMDC monolayers are comparable or even better than that of conventional bulk piezoelectric materials.

Moreover, Zhu *et al.* reported experimental evidence of piezoelectricity in free standing MoS₂ and they found that this material exhibits piezoelectricity for an odd number of layers in which case inversion symmetry is broken.³⁷ Their measured piezoelectric coefficient is 2.9×10^{-10} C/m, which agrees well with recent theoretical calculations.^{31,32} Similarly, by using DFT based theoretical calculations, it has been predicted that group III monodichalcogenides, namely GaS, GaSe and InSe, have piezoelectric stress coefficients of $e_{11} = 1.34 \times 10^{-10}$, 1.34×10^{-10} and 1.47×10^{-10} C/m, respectively.³⁸ In addition, reducing the dimensionality has been shown to enhance piezoelectricity in ZnO.³⁹ These studies indicate that TMDCs are promising candidates as low dimensional piezoelectric materials.

Since previous calculations and experiments were only focused on Mo and W based TMDCs, the potential of other TMDCs and TMDOs for piezoelectric device applications have remained an open question so far. To reveal such potential, first principles calculations are performed in order to systematically investigate the piezoelectric properties of single layer 2H-MX₂ compounds, where M= Cr, Mo, W, Ti, Zr, Hf, Sn and X=O, S, Se, Te. Lattice parameters, atomic positions, electronic band-gap values, elastic stiffness constants (C_{11} and C_{12}), Young modulus (Y), Poisson's ratios (ν), piezoelectric stress coefficients (e_{11}) and piezoelectric strain coefficients (d_{11}) are calculated. The present paper is organized as follows. In section 2, we present our computational methodology. Then, we present the results on electronic properties in section 3, elastic constants in section 4 and piezoelectronic

properties in section 5. Lastly, we conclude briefly in section 6

2 Computational Details

Within the scope of the current study, first-principles calculations based on density functional-theory, as implemented in the Vienna Ab initio Simulation package (VASP) code,^{40,41} are performed. The exchange-correlation interactions are treated using the generalized gradient approximation (GGA) within the Perdew-Burke-Ernzerhof (PBE) formulation^{42,43} and the Heyd-Scuseria-Ernzerhof (HSE06) hybrid functionals.^{44,45} The single electron wave functions are expanded in plane waves with kinetic energy cutoff of 600 eV. For the structure optimizations, the Brillouin-zone integrations are performed using a regular $26 \times 26 \times 1$ k -point mesh within the Monkhorst-Pack scheme.⁴⁶ The convergence criterion for electronic and ionic relaxations are set as 10^{-7} and 10^{-3} eV/Å, respectively. In order to minimize the periodic interaction along the z -direction the vacuum space between the layers is taken at least 15 Å. We checked that a larger vacuum spacing changes the piezoelectric coefficients only by at most 1%. Relaxed- and clamped-ion elastic stiffness coefficients are calculated by the finite difference method as implemented in the VASP code adopting the same first principles parameters used in our previous work.⁴⁷ Piezoelectric stress coefficients, e_{11} are calculated using the Berry Phase approach⁴⁸ as implemented in the VASP package with applied uniform strain, ranging from 0.01 % to -0.01 % in steps of 0.005 %, along the armchair side of the rectangular cell. At this point, in order to apply strain in a desired direction, the hexagonal primitive cell structure of each material is transformed to a tetragonal one composed of two hexagonal primitive cells,³¹ see Fig. 1. A $24 \times 24 \times 1$ k -point mesh is used to calculate the change in polarization.

To investigate the piezoelectric properties of TMDCs and TMDOs, we follow the same theoretical approach of Ref. 31. The piezoelectric tensor,^{49,50} e_{ij} , can be defined in terms of the induced polarization in the direction i due to a strain (ε_j) change along the direction j

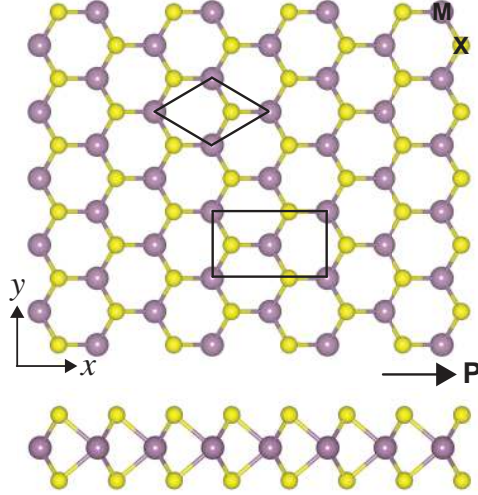


Figure 1: Top and side views of MX_2 where $M = \text{Cr, Mo, W, Ti, Zr, Hf, Sn}$ and $X = \text{O, S, Se, Te}$. P denotes the direction of the polarization. Piezoelectric calculations are done in a rectangular cell.

as follows

$$e_{ij} = \partial P_i / \partial \varepsilon_j = \partial P_i / \partial \varepsilon_j |_{u} + \sum_k (\partial P_i / \partial u_{ik}) (\partial u_{ik} / \partial \varepsilon_j). \quad (1)$$

where P_i is the induced polarization along the direction i as a result of an applied strain along the direction j . The first term in Eq. (1) is the clamped-ion or homogeneous strain contribution to the piezoelectric tensor and it mainly arises from the electronic contribution. The second term represents the contribution from the internal relaxation of ions. Here, u_{ik} is the fractional coordinate of the k^{th} atom along the i direction of the unit cell. Since TMDC and TMDO compounds have a non-centrosymmetric crystal structure, the inclusion of internal relaxation becomes essential in order to obtain realistic piezoelectric properties. In addition, it is clear that the relaxed-ion piezoelectric coefficients are experimentally relevant quantities that can be measured. From the theoretical point of view, since the relaxed-ion piezoelectric coefficients include both electronic and relaxation effects, the calculation of the clamped-ion piezoelectric coefficients helps to separate the electronic and relaxation contributions from the relaxed-ion piezoelectric coefficients. The number of independent piezoelectric tensor coefficient is deduced from the symmetry of the crystal. For TMDCs and TMDOs, we only

need to calculate the e_{11} component of the piezoelectric stress tensor. e_{11} relates in-plane strain to in-plane electrical polarization. The piezoelectric coefficient e_{31} is zero due to the presence of an inversion centre between the two layers of chalcogenides. However, it is found to be non-zero for the unsymmetrical H and F co-decorated graphene.^{51,52} The corresponding piezoelectric strain tensor (d_{11}) of each material is predicted from the following relation:³¹

$$d_{11} = e_{11}/(C_{11} - C_{12}). \tag{2}$$

For each applied strain, the ions are kept in their strained positions or allowed to relax to their new equilibrium positions, and consequently the clamped-ion or relaxed-ion piezoelectric properties are calculated.

At this point, it is worth discussing the experimental realization of the TMDC and TMDO compounds considered in this work. Theoretical calculations suggested that the 2H phase of MoS₂ is energetically more stable than the 1T phase. The latter phase has imaginary vibrational frequencies, which is a sign of instability.¹⁰ However, 1T phase of MoS₂ has been realized recently and was proposed, for instance, as an electrode material together with the 2H phase in MoS₂ based transistors.⁵³ Even though some of the TMDCs and TMDOs considered here have not been synthesized yet in the 2H phase, advances in fabrication techniques will certainly make it possible to fabricate them. The most of the TMDCs based on the group VI elements have been synthesized in 2H form.^{3,6,12,14,17,54,55} Bulk MoTe₂ can also be found in a distorted 1T structure.⁵⁶ In addition, bulk WTe₂ has predominantly a distorted 1T structure.⁵⁶ Since MoTe₂ has been observed in 2H phase, it is expected that the experimental realization of CrTe₂ in the 2H phase is also possible. The phonon calculations and molecular dynamic simulations proved the dynamical stability of single-layer CrS₂.⁵⁷ Ti, Zr and Hf based TMDOs and TMDCs have been shown to be more stable in 1T phase.^{1,2,11,58} However, the calculated heat of formation energies for all TMDCs and TMDOs considered here have been shown to be negative, meaning that these materials

can be sensitized and stabilized by the help of, for instance, a suitable substrate.^{11,59,60}

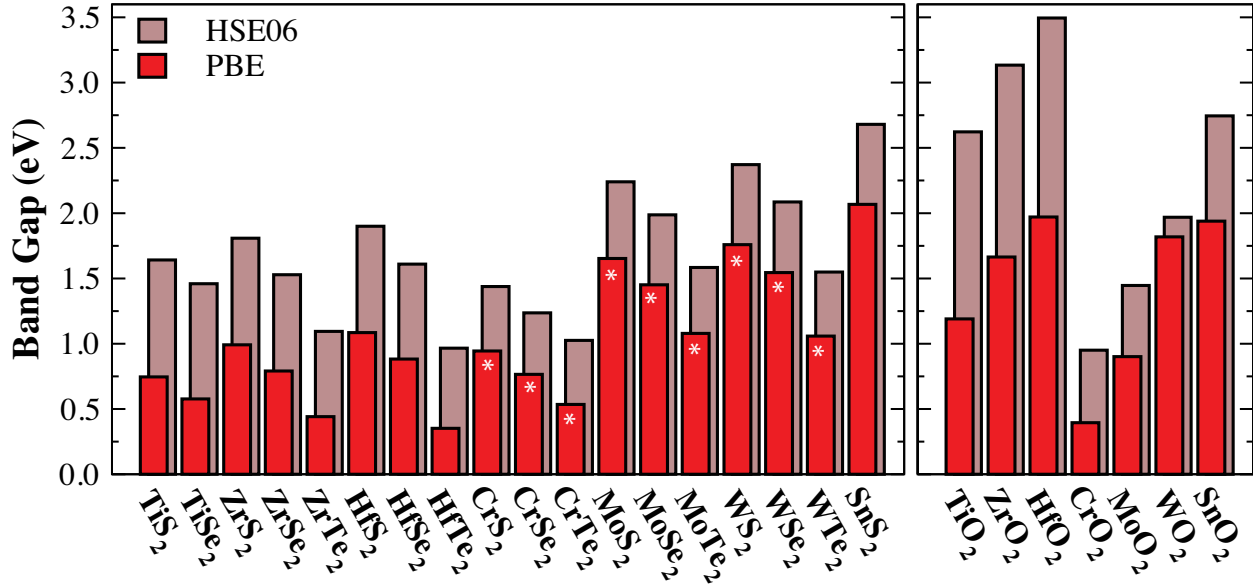


Figure 2: The calculated PBE and HSE06 E_{gap} values for TMDCs and TMDOs. Here, white * sign indicates that it is a direct band gap material.

3 Band gap

It is mandatory that a piezoelectric material has to be an insulator or semiconductor with a sufficiently wide band gap to avoid current leakage. Thus, we first calculate the electronic properties of twenty eight single layer MX_2 compounds, where $M = Cr, Mo, W, Ti, Zr, Hf, Sn$ and $X = O, S, Se, Te$. We discard the metallic structures, namely $SnSe_2, SnTe_2,$ and $TiTe_2$. Actually, G_0W_0 calculations predicted that $2H-TiTe_2$ is a small band gap semiconductor material.¹¹ Since semi-local functionals are used in the Berry's phase calculations, $2H-TiTe_2$ is excluded. For electronic structure calculations, we also applied the HSE06 hybrid functionals in order to obtain realistic electronic band gap values for TMDCs and TMDOs. Figure 2 shows the calculated PBE and HSE06 band gap values. The materials, except Cr, Mo, and W based TMDCs, have indirect band gaps and the predicted values and trends are in good agreement with previous theoretical calculations.^{10,31,32,61} In each metal group, the band gap increases when moving upwards from Te to S.

Table 1: Calculated clamped and relaxed-ion elastic constants (in units of N/m), Young modulus Y (in units of N/m) and Poisson's ratio ν .

Material	Clamped Ion				Relaxed Ion			
	C_{11}	C_{12}	Y	ν	C_{11}	C_{12}	Y	ν
TiS ₂	100.3	34.2	88.6	0.34	89.9	28.6	80.8	0.32
TiSe ₂	84.8	29.3	74.7	0.35	74.4	24.4	66.4	0.33
ZrS ₂	96.3	37.7	81.5	0.39	84.2	31.8	72.2	0.38
ZrSe ₂	83.3	31.0	71.8	0.37	71.4	26.0	61.9	0.36
ZrTe ₂	66.2	22.8	58.35	0.34	53.1	18.6	46.6	0.35
HfS ₂	104.4	39.1	89.8	0.37	92.8	33.8	80.5	0.36
HfSe ₂	89.7	32.2	78.1	0.36	78.8	27.8	69.0	0.35
HfTe ₂	71.0	23.5	63.2	0.33	59.3	19.7	52.8	0.33
CrS ₂	136.9	42.6	123.6	0.31	120.6	32.3	111.9	0.27
CrSe ₂	111.3	37.5	98.7	0.34	96.6	28.9	87.9	0.30
CrTe ₂	86.5	32.7	74.1	0.38	73.0	25.8	63.9	0.30
MoS ₂	157.2	50.1	141.2	0.32	132.7	33.0	124.5	0.25
MoSe ₂	133.2	40.8	120.7	0.31	106.9	25.6	100.8	0.24
MoTe ₂	106.3	32.8	96.2	0.31	84.1	19.8	79.4	0.24
WS ₂	174.7	51.9	159.3	0.30	146.5	31.8	139.6	0.22
WSe ₂	147.4	41.1	135.9	0.28	102.4	23.1	115.9	0.23
WTe ₂	115.4	31.6	106.8	0.27	89.2	15.7	86.4	0.18
SnS ₂	92.8	23.1	87.1	0.25	91.0	22.2	85.6	0.24
TiO ₂	178.9	80.9	142.3	0.45	173.7	75.7	141.7	0.44
ZrO ₂	163.5	83.0	121.5	0.51	157.4	77.5	119.2	0.49
HfO ₂	181.7	86.7	140.3	0.48	174.2	81.5	136.1	0.47
CrO ₂	233.8	87.4	201.1	0.37	218.6	74.4	193.3	0.34
MoO ₂	253.3	104.0	210.6	0.41	230.2	84.5	199.2	0.37
WO ₂	286.2	109.0	244.7	0.38	261.2	87.8	231.7	0.34
SnO ₂	165.7	52.4	149.1	0.32	160.2	53.3	142.5	0.33

4 Elastic constants

As previously mentioned, we need to calculate the elastic constants in order to obtain the piezoelectric strain, d_{11} coefficients, see Eq. (2). Therefore, the relaxed-ion and clamped-ion elastic stiffness coefficients (C_{11} and C_{12}), Young modulus ($Y = (C_{11}^2 - C_{12}^2) / C_{11}$) and Poisson's ratios ($\nu = C_{12} / C_{11}$) for all TMDC and TMDO materials considered in this study are obtained and are listed in Table 1. Our results are in good agreement with available data.^{31,62-64} The first observation from Table 1 is that C_{11} , C_{12} and Y decreases with increase of the row number of the chalcogenide atom. **Except Zr, in each chalcogenide group, the MX_2 monolayer**

becomes stiffer with increase of the row number of the metal atom. Structures considered in this study are found to be less stiff when compared to graphene ($Y=341$ N/m)⁴⁷ and single layer h -BN ($Y=275.9$ N/m).⁴⁷ Also it should be noticed that the calculated elastic constants are positive and satisfy the Born stability criteria for crystals having hexagonal symmetry.^{65,66} Note that the relaxed-ion elastic constants, i.e. C_{11} and C_{12} , are always smaller than the clamped-ion ones since the internal relaxation of ions allows to release some of the stress in the former, see Table 1.

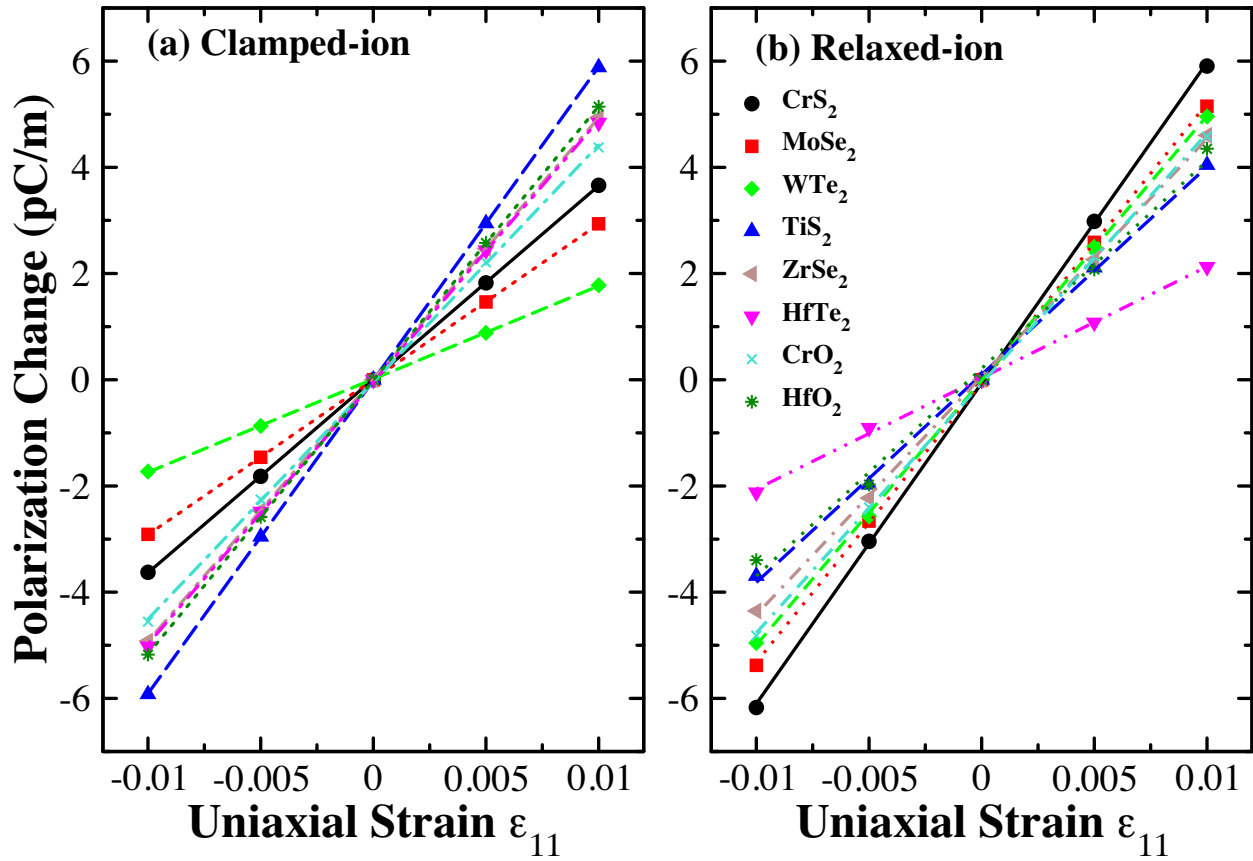


Figure 3: (a) Clamped-ion and (b) relaxed-ion polarization change under applied uniaxial strain (ϵ_{11}) along the x direction for the selected TMDC and TMDO structures. Piezoelectric coefficient is determined from the slope of the curves.

5 Piezoelectric properties

Piezoelectric coefficients (e_{11}) are derived from the slope of the polarization change (Fig. 3) with applied uniform strain, ranging from 0.01 % to -0.01 % in steps of 0.005 %, along the armchair side of the rectangular cell via Berry’s Phase approximation.⁴⁸ The clamped-ion and relaxed-ion d_{11} coefficients are obtained by using the calculated e_{11} coefficients, and the elastic constants (C_{11} and C_{12}) via Eq. (2). Figure 4 shows the calculated e_{11} and d_{11} coefficients for both TMDCs and TMDOs. The materials are ordered along the x -axis by considering the period and group number of the transition metal element in the periodic table. The predicted relaxed-ion e_{11} and d_{11} coefficients are consistent with the available reference data,^{31,57} see results for Cr, Mo and W based TMDCs, which are comparable with the piezoelectric properties of single layer and bulk h -BN.^{31,33–35} In addition, the relaxed-ion e_{11} coefficient of single layer MoS₂ (4.91×10^{-10} C/m) is comparable with the experimentally measured piezoelectric coefficient of 2.90×10^{-10} C/m³⁷ and agrees well with the reported value of 3.64×10^{-10} C/m.³¹ In addition, the trends found for the e_{11} and d_{11} coefficients of Mo and W based TMDCs are consistent with those found in Ref. 31. The difference between our calculated piezoelectric coefficients and previous calculations is likely due to the use of different pseudopotentials, small differences in elastic constants, and other computational parameters (for instance k -mesh).

SnS₂ has the highest e_{11} coefficient for the relaxed-ion (10.7×10^{-10} C/m) calculation. WO₂ has the smallest relaxed-ion piezoelectric stress coefficient (2.49×10^{-10} C/m) among TMDOs and WTe₂ has the smallest clamped-ion piezoelectric stress coefficient (1.75×10^{-10} C/m). From Fig. 4, we predict several periodic trends in clamped-ion e_{11} and d_{11} coefficients for TMDC and TMDO monolayers. The clamped-ion e_{11} coefficients of TMDCs usually increase when moving from right to left in the periodic table (i.e., from CrX₂ to TiX₂) and upward in an individual group of both transition metal and chalcogenide atoms. This trend is nearly the same for TMDOs. However, for TMDCs, the trend (i.e., the increase in the calculated clamped-ion e_{11} coefficients when moving upward in the group of chalcogenide

elements) becomes reversed for the relaxed-ion calculations of group VI elements as clearly seen in Fig. 4(a). The clamped and relaxed ion d_{11} coefficients increase when moving downward in the group of chalcogenide elements (i.e. from S to Te) in each metal group. This trend can be correlated to the polarizability of chalcogenide atoms since the atoms are easily polarized when going downward in a specific group of the periodic table. We notice that the chalcogenide atoms have a much larger impact on the d_{11} coefficients as compared to the metal atoms. Especially in group VI, the d_{11} coefficient is maximized if one uses a smaller metal atom and a larger chalcogenide atom. In group IV, Zr does not exhibit the same trend that is found for the group VI elements. This is partially because the C_{11} elastic constant of Zr based TMDCs for a particular chalcogenide atom is smaller than that of Ti and Hf based TMDCs. Since TMDOs pose larger elastic constants, they usually have smaller d_{11} coefficients as compared to TMDCs. In other words, the stronger the material the smaller the d_{11} coefficient.

Among the group VI elements (i.e., Cr, Mo and W), Cr based TMDCs and TMDOs are found to have much better piezoelectric properties in each chalcogenide group and CrTe_2 possesses the largest relaxed-ion e_{11} (8.06×10^{-10} C/m) and d_{11} (17.1 pm/V) coefficients. On the other hand, the relaxed-ion e_{11} and d_{11} coefficients of SnS_2 are almost the same as those of CrTe_2 . The predicted relaxed-ion e_{11} values are much larger than the values previously predicted for surface decorated graphene structures.⁶⁷ Furthermore, when the piezoelectric coefficients of the extensively used bulk piezoelectric materials, namely 2.3 pm/V for α -quartz,⁶⁸ 3.1 pm/V for wurtzite GaN⁶⁹ and 5.1 pm/V for AlN,⁶⁹ are considered, we predict that TMDCs and TMDOs have comparable or even larger relaxed-ion piezoelectric coefficients.

It is essential to discuss the effect of the internal relaxation on the piezoelectric properties of TMDCs and TMDOs. Relaxing the ion positions after applying strain significantly reduces (increases) the polarization of the Ti, Zr and Hf (Cr, Mo and W) based TMDCs. As a result, the clamped-ion piezoelectric coefficients of the Ti, Zr and Hf (Cr, Mo and W) based TMDCs

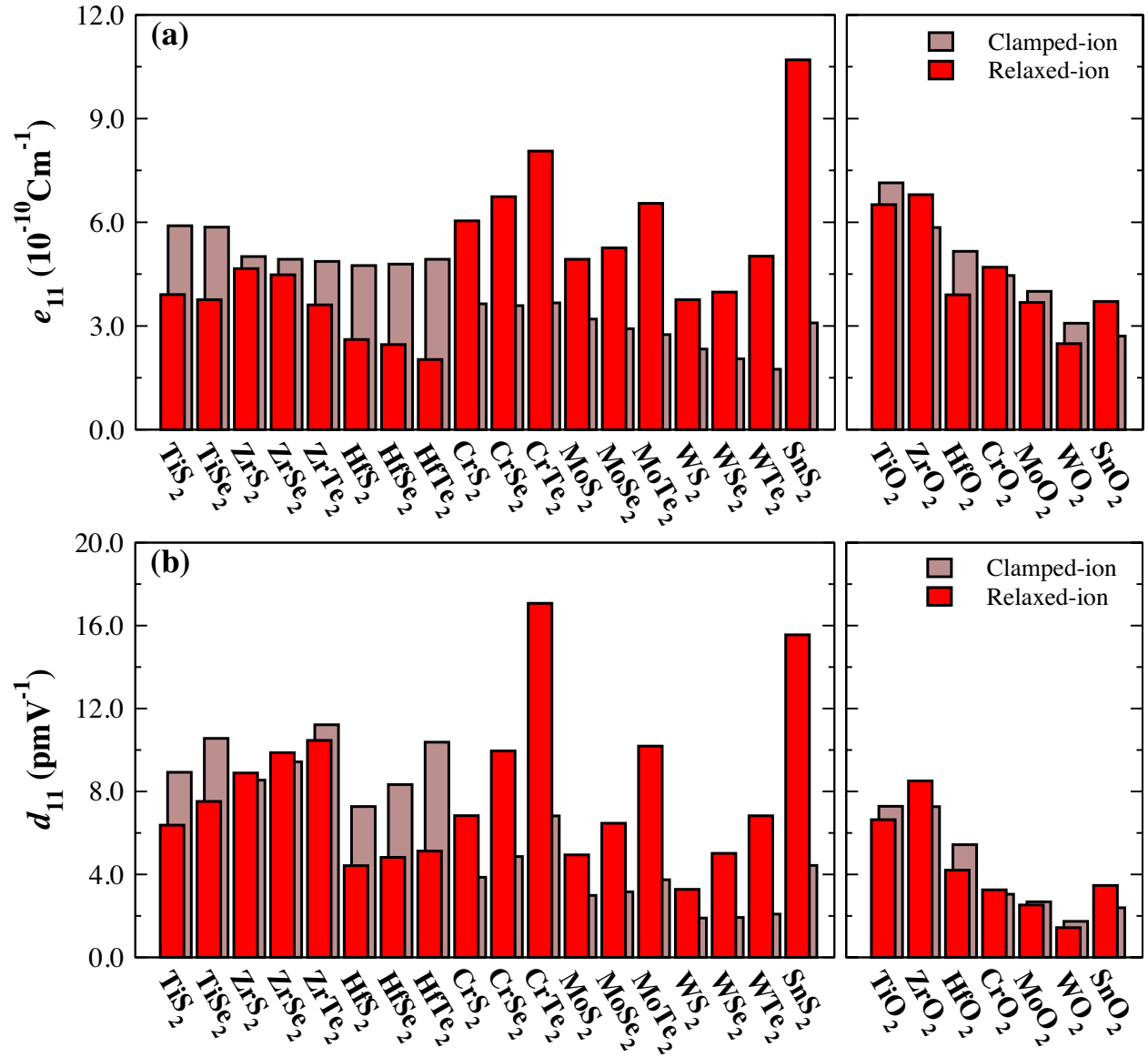


Figure 4: The calculated clamped and relaxed-ion (a) piezoelectric stress (e_{11}) and (b) piezoelectric strain (d_{11}) coefficients.

monolayers are much larger (smaller) than that of the relaxed-ion coefficients. This means that the electronic contribution, i.e. the first term in Eq. (1), and strain contribution, i.e. the second term in Eq. (1), have opposite (the same) sign for the Ti, Zr and Hf (Cr, Mo and W) based TMDCs. The calculated elastic constants suggest that Ti, Zr and Hf based TMDCs are more brittle materials that are expected to exhibit larger response to an applied strain, thereby giving rise to higher clamped-ion piezoelectric constants. For TMDOs, the contribution of internal relaxation to the e_{11} coefficient decrease when moving downward in an individual metal group. However, in each chalcogenide group, the internal relaxation becomes generally less important when going from Te to S. This can be attributed to the large strain-induced ionic motion in response of an applied strain. In other words, after applying strain, the amount of the internal relaxation of the chalcogenide atom increases from S to Te, giving rise to a larger internal relaxation contribution to the piezoelectric coefficients in Te based TMDCs. Since Te is the most easily polarizable atom among the chalcogenide atoms (due to its larger size), the polarization effects (and hence electronic contribution to the e_{11} coefficient) are found to be large in Te based TMDCs as compared to S and Se counterparts. However, the increase in piezoelectricity effects competes with the degradation of stability.

6 Conclusion

In summary, we presented a detailed theoretical investigation of the piezoelectric properties of semiconductor TMDC and TMDO monolayers. Our calculations show that TMDC and TMDO structures are strong candidates for future atomically thin piezoelectric applications. We show that Ti, Zr, Sn and Cr based TMDCs and TMDOs have much better piezoelectric properties as compared to Mo and W based TMDCs and TMDOs and the well-known conventional bulk piezoelectric materials. The usage of these 2D piezoelectric materials in ultra sensitive sensors, low-power electronics and nanoscale electromechanical systems are

expected to have an impact on the size reduction, weight and energy consumption of such devices.

Acknowledgement

M. M. A and C. S. acknowledges the support from Scientific and Technological Research Council of Turkey (TUBITAK-113F333). C.S. acknowledges the support from Anadolu University (BAP-1407F335), and Turkish Academy of Sciences (TUBA-GEBIP). Computational resources were provided by TUBITAK ULAKBIM, High Performance and Grid Computing Center (TR-Grid e-Infrastructure), and HPC infrastructure of the University of Antwerp (CalcUA) a division of the Flemish Supercomputer Center (VSC), which is funded by the Hercules foundation.

References

- (1) Wilson, J.; Yoffe, A. The transition metal dichalcogenides discussion and interpretation of the observed optical, electrical and structural properties. *Advances in Physics* **1969**, *18*, 193–335.
- (2) Klipstein, P. C.; Guy, D. R. P.; Marseglia, E. A.; Meakin, J. I.; Friend, R. H.; Yoffe, A. D. Electronic properties of HfTe₂. *Journal of Physics C: Solid State Physics* **1986**, *19*, 4953.
- (3) Wang, Q. H.; Kalantar-Zadeh, K.; Kis, A.; Coleman, J. N.; Strano, M. S. Electronics and optoelectronics of two-dimensional transition metal dichalcogenides. *Nat. Nanotechnol.* **2012**, *7*, 699.
- (4) Song, X.; Hu, J.; Zeng, H. Two-dimensional semiconductors: recent progress and future perspectives. *J. Mater. Chem. C* **2013**, *1*, 2952.

- (5) Xu, M.; Liang, T.; Shi, M.; Chen, H. Graphene-Like Two-Dimensional Materials. *Chem. Rev.* **2013**, *113*, 3766.
- (6) Huang, X.; Zeng, Z.; Zhang, H. Metal dichalcogenide nanosheets: preparation, properties and applications. *Chem. Soc. Rev.* **2013**, *42*, 1934.
- (7) Chhowalla, M.; Shin Hyeon, S.; Eda, G.; Li, L. J.; Loh, K. P.; Zhang, H. The chemistry of two-dimensional layered transition metal dichalcogenide nanosheets. *Nat. Chem.* **2013**, *5*, 263.
- (8) Jariwala, D.; Sangwan, V. K.; Lauhon, L. J.; Marks, T. J.; Hersam, M. C. Emerging Device Applications for Semiconducting Two-Dimensional Transition Metal Dichalcogenides. *ACS Nano* **2014**, *8*, 1102.
- (9) Lebègue, S.; Björkman, T.; Klintonberg, M.; Nieminen, R. M.; Eriksson, O. Two-Dimensional Materials from Data Filtering and *Ab Initio* Calculations. *Phys. Rev. X* **2013**, *3*, 031002.
- (10) Ataca, C.; Sahin, H.; Ciraci, S. Stable, Single-Layer MX₂ Transition-Metal Oxides and Dichalcogenides in a Honeycomb-Like Structure. *J. Phys. Chem. C* **2012**, *116*, 8983.
- (11) Rasmussen, F. A.; Thygesen, K. S. Computational 2D Materials Database: Electronic Structure of Transition Metal Dichalcogenides and Oxides. *The Journal of Physical Chemistry C* **2015**, *119*, 13169.
- (12) Radisavljevic, B.; Radenovic, A.; Brivio, J.; Giacometti, V.; Kis, A. Single-layer MoS₂ transistors. *Nat. Nano* **2011**, *6*, 147.
- (13) Lee, C.; Yan, H.; Brus, L. E.; Heinz, T. F.; Hone, J.; Ryu, S. Anomalous Lattice Vibrations of Single- and Few-Layer MoS₂. *ACS Nano* **2010**, *4*, 2695.
- (14) Coleman, J. N. et al. Two-Dimensional Nanosheets Produced by Liquid Exfoliation of Layered Materials. *Science* **2011**, *331*, 568.

- (15) Elias, A. L. et al. Controlled Synthesis and Transfer of Large-Area WS₂ Sheets: From Single Layer to Few Layers. *ACS Nano* **2013**, *7*, 5235.
- (16) Gutierrez, H. R.; Perea-Lopez, N.; Elias, A. L.; Berkdemir, A.; Wang, B.; Lv, R.; Lopez-Urias, F.; Crespi, V. H.; Terrones, H.; Terrones, M. Extraordinary Room-Temperature Photoluminescence in Triangular WS₂ Monolayers. *Nano Lett.* **2013**, *13*, 3447.
- (17) Huang, J. K.; Pu, J.; Hsu, C. L.; Chiu, M. H.; Juang, Z. Y.; Chang, Y. H.; Chang, W. H.; Iwasav, Y.; Takenobu, T.; Li, L. J. Large-Area Synthesis of Highly Crystalline WSe₂ Monolayers and Device Applications. *ACS Nano* **2014**, *8*, 923.
- (18) Liu, W.; Kang, J.; Sarkar, D.; Khatami, Y.; Jena, D.; Banerjee, K. Role of Metal Contacts in Designing High-Performance Monolayer n-Type WSe₂ Field Effect Transistors. *Nano Lett.* **2013**, *13*, 1983.
- (19) Mak, K. F.; Lee, C.; Hone, J.; Shan, J.; Heinz, T. F. Atomically Thin MoS₂: A New Direct-Gap Semiconductor. *Phys. Rev. Lett.* **2010**, *105*, 136805.
- (20) Chhowalla, M.; Shin, H. S.; Eda, G.; Li, L.; Loh, K. P.; Zhang, H. The chemistry of two-dimensional layered transition metal dichalcogenide nanosheets. *Nat. Chem.* **2013**, *5*, 263.
- (21) Wang, H.; Feng, H.; Li, J. Graphene and Graphene-like Layered Transition Metal Dichalcogenides in Energy Conversion and Storage. *Small* **2014**, *10*, 2165.
- (22) Jariwala, D.; Sangwan, V. K.; Lauhon, L. J.; Marks, T. J.; Hersam, M. C. Emerging Device Applications for Semiconducting Two-Dimensional Transition Metal Dichalcogenides. *ACS Nano* **2014**, *8*, 1102.
- (23) Larentis, S.; Fallahazad, B.; Tutuc, E. Field-effect transistors and intrinsic mobility in ultra-thin MoSe₂ layers. *Appl. Phys. Lett.* **2012**, *101*, 223104.

- (24) Dankert, A.; Langouche, L.; Kamalakar, M. V.; Dash, S. P. High-Performance Molybdenum Disulfide Field-Effect Transistors with Spin Tunnel Contacts. *ACS Nano* **2014**, *8*, 476.
- (25) Wang, Q. H.; Kalantar-Zadeh, K.; Kis, A.; Coleman, J. N.; Strano, M. S. Electronics and optoelectronics of two-dimensional transition metal dichalcogenides. *Nat. Nano* **2012**, *7*, 699.
- (26) Morten, B.; Deccico, G.; Prudenziati, M. Resonant pressure sensor based on piezoelectric properties of ferroelectric thick films. *Sens. Actuator A-Phys.* **1992**, *31*, 153.
- (27) Jaffe, H.; Berlincourt, D. A. Piezoelectric transducer materials. *Proc IEEE* **1965**, *53*, 1372.
- (28) Wang, Z. L.; Song, J. H. Piezoelectric Nanogenerators Based on Zinc Oxide Nanowire Arrays. *Science* **2006**, *312*, 242.
- (29) Lopez-Suarez, M.; Pruneda, M.; Abadal, G.; Rurali, R. Piezoelectric monolayers as nonlinear energy harvesters. *Nanotechnology* **2014**, *25*, 175401.
- (30) Wu, W.; Wang, L.; Li, Y.; Zhang, F.; Lin, L.; Niu, S.; Chenet, D.; Zhang, X.; Hao, Y.; Heinz, T. F.; Hone, J.; Wang, Z. L. Piezoelectricity of single-atomic-layer MoS₂ for energy conversion and piezotronics. *Nature* **2014**, *514*, 470.
- (31) Duerloo, K. A. N.; Ong, M. T.; Reed, E. J. Intrinsic Piezoelectricity in Two-Dimensional Materials. *J. Phys. Chem. Lett.* **2012**, *3*, 2871.
- (32) Tunghathathip, N.; Bovornratanaraks, T.; Phaisangittisakul, N. Calculation of Piezoelectric Coefficients for Monolayer of Boron Nitride and Transition Metal Dichalcogenides Using Density Functional Theory. *Thai J. Phys.* **2014**, *10*, 17002.
- (33) Michel, K. H.; Verberck, B. Theory of elastic and piezoelectric effects in two-dimensional hexagonal boron nitride. *Phys. Rev. B* **2009**, *80*, 224301.

- (34) Michel, K. H.; Verberck, B. Phonon dispersions and piezoelectricity in bulk and multilayers of hexagonal boron nitride. *Phys. Rev. B* **2011**, *83*, 115328.
- (35) Michel, K. H.; Verberck, B. Theory of phonon dispersions and piezoelectricity in multilayers of hexagonal boron-nitride. *physica status solidi (b)* **2011**, *248*, 2720.
- (36) Zelisko, M.; Hanlummyuang, Y.; Yang, S.; Liu, Y.; Lei, C.; Li, J.; Ajayan, P. M.; Sharma, P. Anomalous piezoelectricity in two-dimensional graphene nitride nanosheets. *Nat. Commun.* **2014**, *5*, 4284.
- (37) Zhu, H.; Wang, Y.; Xiao, J.; Liu, M.; Xiong, S.; Wong, Z. J.; Ye, Z.; Ye, Y.; Yin, X.; Zhang, X. Observation of piezoelectricity in free-standing monolayer MoS₂. *Nat. Nano* **2015**, *10*, 151.
- (38) Li, W.; Li, J. Piezoelectricity in Two-Dimensional Group III Monochalcogenides. *arXiv:1503.07379 [cond-mat.mtrl-sci]* **2015**,
- (39) Xiang, H. J.; Yang, J.; Hou, J. G.; Zhu, Q. Piezoelectricity in ZnO nanowires: A first-principles study. *Applied Physics Letters* **2006**, *89*, 223111.
- (40) Kresse, G.; Hafner, J. Ab initio molecular dynamics for liquid metals. *Phys. Rev. B* **1993**, *47*, 558.
- (41) Wu, X.; Vanderbilt, D.; Hamann, D. R. Systematic treatment of displacements, strains, and electric fields in density-functional perturbation theory. *Phys. Rev. B* **2005**, *72*, 035105.
- (42) Perdew, J. P.; Burke, K.; Ernzerhof, M. Generalized Gradient Approximation Made Simple. *Phys. Rev. Lett.* **1996**, *77*, 3865.
- (43) Perdew, J. P.; Burke, K.; Ernzerhof, M. Generalized Gradient Approximation Made Simple. *Phys. Rev. Lett.* **1996**, *77*, 3865.

- (44) Heyd, J.; Scuseria, G.; Ernzerhof, M. Hybrid functionals based on a screened Coulomb potential. *J. Chem. Phys.* **2003**, *118*, 8207.
- (45) Fuchs, F.; Furthmüller, J.; Bechstedt, F.; Shishkin, M.; Kresse, G. Quasiparticle band structure based on a generalized Kohn-Sham scheme. *Phys. Rev. B* **2007**, *76*, 115109.
- (46) Monkhorst, H. J.; Pack, J. D. Special points for Brillouin-zone integrations. *Phys. Rev. B* **1976**, *13*, 5188.
- (47) Çakır, D.; Peeters, F. M.; Sevik, C. Mechanical and thermal properties of h -MX₂ (M=Cr, Mo, W; X=O, S, Se, Te) monolayers: A comparative study. *Appl. Phys. Lett.* **2014**, *104*, 203110.
- (48) Vanderbilt, D. Berry-phase theory of proper piezoelectric response. *J. Phys. Chem. Solids* **2000**, *61*, 147.
- (49) Baroni, S.; de Gironcoli, S.; Dal Corso, A.; Giannozzi, P. Phonons and related crystal properties from density-functional perturbation theory. *Rev. Mod. Phys.* **2001**, *73*, 515–562.
- (50) Wu, X.; Vanderbilt, D.; Hamann, D. R. Systematic treatment of displacements, strains, and electric fields in density-functional perturbation theory. *Phys. Rev. B* **2005**, *72*, 035105.
- (51) Ong, M. T.; Duerloo, K.-A. N.; Reed, E. J. The Effect of Hydrogen and Fluorine Coadsorption on the Piezoelectric Properties of Graphene. *The Journal of Physical Chemistry C* **2013**, *117*, 3615–3620.
- (52) Kim, H. J.; Noor-A-Alam, M.; Son, J. Y.; Shin, Y.-H. Origin of piezoelectricity in monolayer halogenated graphane piezoelectrics. *Chemical Physics Letters* **2014**, *603*, 62 – 66.

- (53) Kappera, R.; Voiry, D.; Yalcin, S. E.; Branch, B.; Gupta, G.; Mohite, A. D.; Chhowalla, M. Phase-engineered low-resistance contacts for ultrathin MoS₂ transistors. *Nat Mater* **2014**, *13*, 1128–1134.
- (54) Zhang, X.; Xie, Y. Recent advances in free-standing two-dimensional crystals with atomic thickness: design, assembly and transfer strategies. *Chem. Soc. Rev.* **2013**, *42*, 8187–8199.
- (55) Lee, Y.-H.; Zhang, X.-Q.; Zhang, W.; Chang, M.-T.; Lin, C.-T.; Chang, K.-D.; Yu, Y.-C.; Wang, J. T.-W.; Chang, C.-S.; Li, L.-J.; Lin, T.-W. Synthesis of Large-Area MoS₂ Atomic Layers with Chemical Vapor Deposition. *Advanced Materials* **2012**, *24*, 2320–2325.
- (56) Brown, B. E. The crystal structures of WTe₂ and high-temperature MoTe₂. *Acta Crystallographica* **1966**, *20*, 268–274.
- (57) Zhuang, H. L.; Johannes, M. D.; Blonsky, M. N.; Hennig, R. G. Computational prediction and characterization of single-layer CrS₂. *Applied Physics Letters* **2014**, *104*, 022116.
- (58) Guo, H.; Lu, N.; Wang, L.; Wu, X.; Zeng, X. C. Tuning Electronic and Magnetic Properties of Early Transition-Metal Dichalcogenides via Tensile Strain. *The Journal of Physical Chemistry C* **2014**, *118*, 7242–7249.
- (59) Wang, Y. et al. Monolayer PtSe₂, a New Semiconducting Transition-Metal-Dichalcogenide, Epitaxially Grown by Direct Selenization of Pt. *Nano Letters* **2015**, *15*, 4013–4018, PMID: 25996311.
- (60) Singh, A. K.; Zhuang, H. L.; Hennig, R. G. *Ab initio* synthesis of single-layer III-V materials. *Phys. Rev. B* **2014**, *89*, 245431.

- (61) Guo, H.; Lu, N.; Wang, L.; Wu, X.; Zeng, X. C. Tuning Electronic and Magnetic Properties of Early Transition-Metal Dichalcogenides via Tensile Strain. *J. Phys. Chem. C* **2014**, *118*, 7242.
- (62) Peng, Q.; De, S. Outstanding mechanical properties of monolayer MoS₂ and its application in elastic energy storage. *Phys. Chem. Chem. Phys.* **2013**, *15*, 19427.
- (63) Kang, J.; Tongay, S.; Zhou, J.; Li, J.; Wu, J. Band offsets and heterostructures of two-dimensional semiconductors. *Appl. Phys. Lett.* **2013**, *102*, 012111.
- (64) Cooper, R. C.; Lee, C.; Marianetti, C. A.; Kysar, J. W. Nonlinear elastic behavior of two-dimensional molybdenum disulfide. *Phys. Rev. B* **2013**, *87*, 035423.
- (65) Nye, J. F. *Physical properties of Crystals, Their representation by Tensors and Matrices*; Clarendon Press: Oxford, 1957.
- (66) Born, M.; Huang, K. *Dynamical Theory of Crystal Lattices*; Oxford University Press: Oxford, 1988.
- (67) Ong, M. T.; Reed, E. J. Engineered Piezoelectricity in Graphene. *ACS Nano* **2012**, *6*, 1387.
- (68) Behmann, R. Elastic and Piezoelectric Constants of Alpha-Quartz. *Phys. Rev.* **1958**, *110*, 1060.
- (69) Lueng, C. M.; Chan, H. L. W.; Surya, C.; Choy, C. L. Piezoelectric coefficient of aluminum nitride and gallium nitride. *J. Appl. Phys.* **2000**, *88*, 5360.